

2015-09-02

On the application of a hybrid ellipsoidal-rectangular interval arithmetic algorithm to interval Kalman filtering for state estimation of uncertain systems

Motwani, A

<http://hdl.handle.net/10026.1/3639>

10.1080/00207179.2015.1018951

International Journal of Control

Informa UK Limited

All content in PEARL is protected by copyright law. Author manuscripts are made available in accordance with publisher policies. Please cite only the published version using the details provided on the item record or document. In the absence of an open licence (e.g. Creative Commons), permissions for further reuse of content should be sought from the publisher or author.



International Journal of Control

Publication details, including instructions for authors and subscription information:
<http://www.tandfonline.com/loi/tcon20>

On the application of a hybrid ellipsoidal-rectangular interval arithmetic algorithm to interval Kalman filtering for state estimation of uncertain systems

Amit Motwani^a, Sanjay Sharma^a, Robert Sutton^a & Philip Culverhouse^a

^a School of Marine Science and Engineering, Plymouth University, Plymouth, UK

Accepted author version posted online: 13 Feb 2015.



[Click for updates](#)

To cite this article: Amit Motwani, Sanjay Sharma, Robert Sutton & Philip Culverhouse (2015): On the application of a hybrid ellipsoidal-rectangular interval arithmetic algorithm to interval Kalman filtering for state estimation of uncertain systems, International Journal of Control, DOI: [10.1080/00207179.2015.1018951](https://doi.org/10.1080/00207179.2015.1018951)

To link to this article: <http://dx.doi.org/10.1080/00207179.2015.1018951>

Disclaimer: This is a version of an unedited manuscript that has been accepted for publication. As a service to authors and researchers we are providing this version of the accepted manuscript (AM). Copyediting, typesetting, and review of the resulting proof will be undertaken on this manuscript before final publication of the Version of Record (VoR). During production and pre-press, errors may be discovered which could affect the content, and all legal disclaimers that apply to the journal relate to this version also.

PLEASE SCROLL DOWN FOR ARTICLE

Taylor & Francis makes every effort to ensure the accuracy of all the information (the "Content") contained in the publications on our platform. However, Taylor & Francis, our agents, and our licensors make no representations or warranties whatsoever as to the accuracy, completeness, or suitability for any purpose of the Content. Any opinions and views expressed in this publication are the opinions and views of the authors, and are not the views of or endorsed by Taylor & Francis. The accuracy of the Content should not be relied upon and should be independently verified with primary sources of information. Taylor and Francis shall not be liable for any losses, actions, claims, proceedings, demands, costs, expenses, damages, and other liabilities whatsoever or howsoever caused arising directly or indirectly in connection with, in relation to or arising out of the use of the Content.

This article may be used for research, teaching, and private study purposes. Any substantial or systematic reproduction, redistribution, reselling, loan, sub-licensing, systematic supply, or distribution in any form to anyone is expressly forbidden. Terms & Conditions of access and use can be found at <http://www.tandfonline.com/page/terms-and-conditions>

Publisher: Taylor & Francis

Journal: *International Journal of Control*

DOI: <http://dx.doi.org/10.1080/00207179.2015.1018951>

On the application of a hybrid ellipsoidal-rectangular interval arithmetic algorithm to interval Kalman filtering for state estimation of uncertain systems

Amit Motwani^{a,*}, Sanjay Sharma^a, Robert Sutton^a, Philip Culverhouse^b

^aSchool of Marine Science and Engineering, Plymouth University, Plymouth, UK

^bSchool of Computing and Mathematics, Plymouth University, Plymouth, UK

Author information:

Amit Motwani. Postal address: Room 001, Buckland House, Drake Circus, Plymouth, Devon, PL4 8AA, U.K. Telephone: +44 (0) 7411103738. Email: amit.motwani@plymouth.ac.uk

Professor Robert Sutton. Postal address: Reynolds building, Drake Circus, Plymouth, Devon, PL4 8AA, U.K. Telephone: +44(0)1752586151. Email: R.Sutton@plymouth.ac.uk

Dr Sanjay Sharma. Postal address: Room 101, Reynolds, Drake Circus, Plymouth, Devon, PL4 8AA, U.K. Telephone: +44(0) 1752586147. Email: sanjay.sharma@plymouth.ac.uk

Associate Professor Phil Culverhouse. Postal address: A323, 22 Portland Square, Drake Circus, Plymouth, Devon, PL4 8AA, U.K. Email: P.Culverhouse@plymouth.ac.uk

*Corresponding author. Email: amit.motwani@plymouth.ac.uk

This work was supported by the EPSRC under Grant EP/I012923/1.

Manuscript word count (exclusive of references and figure captions): 4888 words.

Modelling uncertainty is a key limitation to the applicability of the classical Kalman filter for state estimation of dynamic systems. For such systems with bounded modelling uncertainty, the interval Kalman filter (IKF) is a direct extension of the former to interval systems. However, its usage is not yet widespread owing to the over-conservatism of interval arithmetic bounds. In this paper, the IKF equations are adapted to use an ellipsoidal arithmetic that, in some cases, provides tighter bounds than direct, rectangular interval arithmetic. In order for the IKF to be useful, it must be able to provide reasonable enclosures under all circumstances. To this end, a hybrid ellipsoidal-rectangular enclosure algorithm is proposed, and its robustness is evidenced by its application to two characteristically different systems for which it provides stable estimate bounds, whereas the rectangular and ellipsoidal approaches fail to accomplish this in either one or the other case.

Keywords: interval Kalman filtering; ellipsoidal arithmetic; robust state estimation

1. Introduction

State estimation has been a topic of investigation for many years, with the Kalman filter (KF) (Kalman, 1960) being the most prominent example of a technique that has achieved widespread usage in the case of linear systems with stochastic uncertainty, owing to its optimality and ease of implementation. Modifications to this scheme have been developed over the years for the non-linear case, relaxed noise assumptions, etc. (Julier and Uhlmann, 1997; Smith, Schmidt, and McGee, 1961; Wu and Chen, 1999).

However, the KF operates under the strict assumption of complete knowledge of the system dynamical model, which in many situations, if not most, constitutes a serious practical limitation. This has led to research on robust state estimation, which aims to obtain estimates of unmeasurable state variables when the system model is only known with some degree of precision.

Most of the research in the field of robust state estimation for uncertain systems has centred on the guaranteed cost state paradigm, the set-valued estimation approach, and robust H_∞ filtering. The first of these is sometimes regarded as an extension of the KF to uncertain systems, and called robust Kalman filtering. The approach is to construct a state estimator that bounds the mean square estimation error by establishing an upper bound on the state estimation error covariance (Jain, 1975; Petersen and McFarlane, 1996). The set-valued estimation approach is based on the deterministic interpretation of Kalman filtering obtained by describing the noise processes as norm bounded (Bertsekas & Rhodes, 1971), and then finding the set in the state space that is consistent with the observed measurements via set inversion, usually requiring some optimisation algorithm (Jaulin, 2009; Savkin and Petersen, 1998; Zhu, 2012). H_∞ filtering centres on minimising the H_∞ norm of the transfer function from the disturbance inputs to the estimation error, and in the case of robust H_∞ filtering, aims to minimise the worst case H_∞ norm (Gao and Chen 2007; Sayed 2001).

All the aforementioned approaches involve a modification or extension of the KF algorithm. However, another approach is to directly use the KF on uncertain models. The method proposed by Chen, Wang, and Shieh (1997), the so called interval KF (IKF), is actually not a modification of the KF at all: as will be shown, its equations exactly mirror those of the traditional KF. In order for the filter to have the same equations, the model it operates on must have exactly the same form as required for a KF. The difference, in this case, is in the type of element set it is constructed upon: rather than the set of real numbers \mathbb{R} , the IKF assumes elements to belong to the set of nonempty, closed and bounded real intervals, \mathbb{IR} . This allows for a natural description of bounded uncertainty to be incorporated into any model without necessitating any additional morphological description. The IKF retains all the same optimal properties of

the standard KF, naturally providing guaranteed bounds to the optimal state estimate by giving these as interval-valued elements.

Despite the seeming simplicity and advantage of this approach, the IKF has seen very limited acceptance since its conception, with only a few authors suggesting its usage for practical applications (He and Vik, 1999; Siouris, Chen, and Wang, 1997; Tiano, Zirilli, and Pizzocchero, 2001; Tiano, Zirilli, Cuneo, and Pagnan, 2005). One of the main reasons being that the IKF requires the use of interval arithmetic (IA), which can be difficult to implement successfully in practice owing to its overly conservative nature, resulting in very large over-estimations of the set of states of the interval system, as will be shown in this paper. The intention of this study is to develop a method that enables efficient computation of the IKF states so that these may be used as was intended by Chen and co-authors.

Although there have been several studies aimed at surmounting the practical difficulties of implementing the IKF owing to the aforementioned overestimation, they typically find ways to reduce the estimation set enclosures to more useful ones, leading to a loss of the guaranteed bounds to the optimal state estimate that the IKF provides (Ahn, Kim, and Chen, 2012; Weng, Chen, Shieh, and Larsson, 2000). In contrast, this paper aims to find “tight” enclosures but always to the actual set of estimates that would be obtained if IA could be carried out with infinite tightness, thus without losing the guarantee of containing the optimal KF estimate.

The layout of the paper is as follows. Section 2 motivates the need for robust estimation by illustrating the inadequacy of the standard KF when an incorrect dynamical system model is used by the filter, which in turn leads to the concept of the interval model as that which can fully describe the uncertain, but bounded, knowledge of the system dynamics. This is followed by an explanation, in Section 3, of why direct

application of IA yields over-conservative results. Section 4 outlines the ellipsoidal arithmetic used and shows that it is not always advantageous, based on which a hybrid ellipsoidal-rectangular enclosure algorithm is developed. Section 5 adapts the IKF equations as affine transformations in order to be able to apply ellipsoidal arithmetic, and the application of the hybrid enclosure method is then applied to interval Kalman filtering on two different systems with different dynamic characteristics in order to illustrate the robustness of the method. Finally conclusions are given in Section 7.

2. Interval Kalman filtering for state estimation of stochastic systems with bounded parametric uncertainty

Consider a dynamic system modelled in discrete-time via the following stochastic state-space equations

$$x(k+1) = A x(k) + B u(k) + \omega(k) \quad (1)$$

$$y(k) = C x(k) + v(k) \quad (2)$$

with

$$A = \begin{bmatrix} 0.8 & -0.2225 \\ 1 & 0 \end{bmatrix}, B = \begin{bmatrix} 1 \\ 0 \end{bmatrix}, C = [0 \quad 0.4225], \omega \sim N(0, Q), Q = \text{cov}(\omega) = 0.01 \times \text{diag}\{1, 1\}, v = N(0, R), R = 4 \quad (3)$$

where $x(k)$ is the system state at time k , $u(k)$ is a controllable system input, $\omega(k)$ is a random input disturbance, and $y(k)$ represents a noisy measurement of the system output, $v(k)$ being the measurement noise. If $\{x(0), \omega(0), \dots, \omega(k), v(0), \dots, v(k)\}$ are mutually independent, then Kalman filtering provides a statistically optimal estimate of the state vector at each time-step.

KF equations:

Prediction:

$$\hat{x}(k|k-1) = A \hat{x}(k-1|k-1) + B u(k-1) \quad (4)$$

$$P(k|k-1) = A P(k-1|k-1) A^T + Q \quad (5)$$

Kalman gain:

$$K(k) = P(k|k-1) C^T \{C P(k|k-1) C^T + R\}^{-1} \quad (6)$$

Correction:

$$\hat{x}(k|k) = \hat{x}(k|k-1) + K(k) \{y(k) - C \hat{x}(k|k-1)\} \quad (7)$$

$$P(k|k) = \{I - K(k) C\} P(k|k-1) \quad (8)$$

However, the optimality of the KF relies on precise knowledge of the system dynamical model (Motwani, Sharma, Sutton, and Culverhouse, 2013).

To illustrate this point, consider a set-point tracking problem in which the system is controlled via a state-feedback control law according to

$$u(k) = -K_c x(k) + K_s y_r(k) \quad (9)$$

where K_c is the vector of state-feedback gains, K_s is a scaling gain calculated to ensure that the overall steady-state closed-loop gain is unity, and y_r is a prescribed reference target for the system output. Let K_c be chosen so that the closed-loop step-response has zero overshoot (or unit damping), and a rise-time (0 to 90%) of $k < 5$, for which a dominant closed-loop pole at 0.6 and a fast pole at 0.1 suffice, requiring a value of $K_c = [0.1, -0.1625]$ and $K_s \approx 0.852$ (note that this control law is used by way of example to generate a realistic stabilising input $u(k)$, but for the sole purpose of state-estimation, any other input could be prescribed instead).

A simulation of the system is carried out for one hundred time-steps, with the initial state being zero, and the target y_r being set at 20, 50 and -15 for each one-third of the simulation respectively. The disturbance and measurement noise sequences are generated pseudo randomly according to the statistics given in (3). The state trajectory of the system is then shown in Figure 1, and the output in Figure 2. Also shown in the two figures are the KF estimates of the system state and output, for the same control input, disturbance input, and output noise sequences, in which the model parameters used by the filter have been overestimated by 5%. The KF initial estimate was taken equal to the true initial state, and the initial error covariance as zero. One can clearly observe that the KF estimates are biased due to the modelling error.

In practice, 100 percent accurate system modelling is utopian: at best, even in the case of modelling via a first-principles approach, small modelling errors exist because values of physical parameters (mass, geometry, resistivity, permittivity, absorbance, etc.) can only be measured with a finite tolerance, not to mention that such parameters are often sensitive to variable external factors, such as temperature, etc. Tolerances, though, provide bounds to the models obtained.

If model parameters cannot be known with absolute precision, but bounds to these are known, then the idea of describing system dynamics with interval values arises naturally, ensuing in an interval model:

$$x(k+1) = A^I x(k) + B^I u(k) + \omega(k) \quad (10)$$

$$y(k) = C^I x(k) + v(k) \quad (11)$$

in which A^I , B^I and C^I are interval-valued matrices, that is, their elements are made up of bounded intervals, i.e. elements of the form

$$m_{i,j}^I = [m_{i,j}^{min}, m_{i,j}^{max}]; \text{ with } m_{i,j}^{min}, m_{i,j}^{max} \in \Re \quad (12)$$

so that they can be written as

$$A^I = A \pm \Delta A = [A - \Delta A, A + \Delta A] \quad (13)$$

$$B^I = B \pm \Delta B = [B - \Delta B, B + \Delta B] \quad (14)$$

$$C^I = C \pm \Delta C = [C - \Delta C, C + \Delta C] \quad (15)$$

where A , B and C represent some nominal point-valued model.

In the late nineties a KF applied to interval system models was proposed by Chen et al. (1997). Chen et al. leveraged the properties of an IA defined by Moore three decades earlier (Moore, 1966). One of the basic tenets of Moore's IA was that calculations involving interval values must enclose every possible result that can be obtained by operating on individual point-values contained within these. The resulting interval thus guarantees bounds to the resulting set, though it may not equal it (a quality known as the *inclusion property*). Using an extension of habitual statistical properties to interval matrices and functions, Chen et al. constructed the IKF, whose equations ((16) to (20)) mimic those of the ordinary KF, but provides state estimates in the form of interval values.

IKF equations:

Prediction:

$$\hat{x}^I(k|k-1) = A^I \hat{x}^I(k-1|k-1) + B^I u(k-1) \quad (16)$$

$$P^I(k|k-1) = A^I P(k-1|k-1) A^{IT} + Q \quad (17)$$

Kalman gain:

$$K^I(k) = P^I(k|k-1) C^{IT} \{C^I P^I(k|k-1) C^{IT} + R\}^{-1} \quad (18)$$

Correction:

$$\hat{x}^I(k|k) = \hat{x}^I(k|k-1) + K^I(k) \{y(k) - C^I \hat{x}^I(k|k-1)\} \quad (19)$$

$$P^I(k|k) = \{I - K^I(k) C^I\} P^I(k|k-1) \quad (20)$$

Note that the state and error covariance estimates, as well as the Kalman gain, are now interval-valued; however $y(k)$ is point-valued as it is a measurement of the (true, not interval) output obtained via some sensor(s). The IKF, statistically optimal in the same sense as the ordinary KF, provides interval state estimates which guarantee to contain the KF estimates of every possible point-valued system contained in the interval model, a consequence of the aforementioned inclusion property of IA. That is, it allows the bounded uncertainty of the system model to be translated into bounds for the optimal state estimates.

3. The wrapping effect

Assume that in the model (1) to (3) the elements of A, B, and C are known only to within 5% of the given values. Then the interval model (10) to (11), with

$$A^I = A \pm 0.05 |A| = [A - 0.05 |A|, A + 0.05 |A|] \quad (21)$$

$$B^I = B \pm 0.05 |B| = [B - 0.05 |B|, A + 0.05 |B|] \quad (22)$$

$$C^I = C \pm 0.05 |C| = [C - 0.05 |C|, A + 0.05 |C|] \quad (23)$$

bounds the actual dynamics of the system, and the IKF estimates guarantee to contain the optimal KF estimates of the system state (Chen et al., 1997). Based on the same

inputs $u(k)$ used in the previous simulation, and an initial state vector and error covariance given by

$$\hat{x}^I(0) = \begin{bmatrix} [-0.005, 0.005] \\ [-0.005, 0.005] \end{bmatrix}; \quad P^I(0) = \begin{bmatrix} [0,0] & [0,0] \\ [0,0] & [0,0] \end{bmatrix} \quad (24)$$

the upper and lower bounds of the IKF estimate of the output, $C^I \hat{x}^I(k)$, are shown in Figure 3, along with the actual output $y(k)$. The IA was carried out in MATLAB using the IA package known as INTerval LABoratory (INTLAB), developed by Rump (1999).

One thing is clearly apparent from observation of the figure: the widths of the IKF interval-estimates expand exponentially, leading to bounds of the estimate that lose any practical value. Moreover the figure only depicts the simulation of the IKF until $k = 57$: estimates of the bounds for $k = 60$ and above were not possible as they surpassed the maximum and minimum IEEE 754 double precision floating point representation ($\approx 1.8 \times 10^{308}$).

One of the problems with IA is that direct computation yields over-conservative results as a consequence of the inclusion property. This can be seen with a simple example: consider an interval value $a^I = [-a, a]$, $a \in \mathfrak{R}$ and $b \in \mathfrak{R}$, then

$$\begin{aligned} a^I \times (b - b) &= a^I \times b - a^I \times b = [-a, a] \times b - [-a, a] \times b = [-a \times b, a \times b] - \\ &[-a \times b, a \times b] = [-2a \times b, 2a \times b] \end{aligned} \quad (25)$$

however, clearly the exact solution set is the single number zero. The overestimation occurs because, after expansion of the brackets in the initial product, the arithmetic does not remember that the interval variable a^I in both terms represent the same variable. In

the case of operations including interval vectors, the memory-less nature of IA has a more severe effect.

Consider an interval vector $x^I = \begin{bmatrix} [-3, 3] \\ [-1, 1] \end{bmatrix}$, which can be represented as a rectangle (Figure 4), and the rotation matrix $A = \begin{bmatrix} \cos(\alpha) & -\sin(\alpha) \\ \sin(\alpha) & \cos(\alpha) \end{bmatrix}$, $\alpha = 20 \times \frac{\pi}{180}$. Then $x^I := A x^I$ represents the anticlockwise rotation of this rectangle by the angle α (20°). Upon performing this operation using IA, the resultant enclosure is not the rotated rectangle, but a rectangle with sides parallel to the coordinate axes that encloses the former, which is consistent with the memory-less nature of IA described earlier, since the correlation between the two dimensions given by the set of individually rotated points is lost. The visual interpretation of this consequence has resulted in its being known as *the wrapping effect* (Neumaier, 1993). The left column of Figure 4 depicts this process, first for a single rotation, and then ten successive applications of the same, evidencing the ever-growing volume of the resulting rectangle; whereas the actual transformed set is always the same size, given the volume preserving nature of A , which is an orthogonal matrix. This process clearly shows that direct application of IA can be overly-conservative. However, as shown in the right column of Figure 4, if the initial rectangle is first enclosed by an ellipse, then each successive rotation of the ellipse does not need to be “wrapped” before a successive rotation is applied, since ellipses are preserved under rotations, and in general, ellipsoids under affine transformations. Indeed, let X be the set of points of the ellipsoid $E(z, L, r)$ $:= \{z + L \xi : \xi \in \mathbb{R}^n, \|\xi\| \leq r\}$, $z \in \mathbb{R}^n$, $L \in \mathbb{R}^{n \times n}$, $r \in \mathbb{R}_+$, then, the set of points transformed by the affinity $x := A x + b$, $A \in \mathbb{R}^{n \times n}$, $x, b \in \mathbb{R}^n$, is given by the ellipsoid $E(\bar{z}, \bar{L}, r)$, with $\bar{z} = A z + b$ and $\bar{L} = A L$.

4. A hybrid ellipsoidal-rectangular IA enclosure algorithm for recursive interval affine transformations

In the previous section, the advantage of using ellipsoidal arithmetic over (rectangular) IA for recursive affine transformations of sets in order to avoid the wrapping effect was made apparent. However, whilst ellipsoids are conserved under affine transformations, they are not so under interval transformations. In the case of an interval affine transformation, $x := A^I x + b^I$, a practicable ellipsoidal enclosure to the set of transformed points must be sought. Neumaier (1993) has developed a method that guarantees such an enclosure with a certain degree of optimality. The main results of this method are summarised next.

Let X be the set of points of the ellipsoid $E(z, L, r) := \{z + L \xi : \xi \in \mathbb{R}^n, \|\xi\| \leq r\}$, $z \in \mathbb{R}^n$, $L \in \mathbb{R}^{n \times n}$, $r \in \mathbb{R}_+$, and $x := A x + b$, $A \in A^I$, $b \in b^I$ an interval affine transformation of $x \in \mathbb{R}^n$, with A^I and b^I an $n \times n$ and $n \times 1$ interval-valued matrix and vector respectively. Neumaier shows that for any $\bar{z} \in \mathbb{R}^n$, $\bar{L} \in \mathbb{R}^{n \times n}$, if $\tilde{r} = \|\bar{L}^{-1}(A^I \bar{z} + b^I - z)\| + \|\bar{L}^{-1} A^I \bar{L}\| r$, then $A x + b \in E(\bar{z}, \bar{L}, \tilde{r}) \quad \forall A \in A^I, b \in b^I, x \in X$. This allows one to find an (ellipsoidal) enclosure for the interval affine transformed points of X , but such enclosure may by no means be “tight”.

However, let $\bar{z} = \text{mid}(A^I z + b^I)$, $d = |A^I z + b^I - z|$, $B = \text{mid}(A^I L)$, and $d' = \nu(A^I L - B)$, where ν is the Frobenius norm. Then, for any non-singular \bar{L} and any non-singular diagonal matrix D , it can be verified that $\tilde{r} \leq \|\bar{L}^{-1} B\| r + \|\bar{L}^{-1} D\| q$, where $q = \|D^{-1} d\| + \|D^{-1} d'\| r$. In particular, for an \bar{L} that satisfies $r^2 B B^T + q^2 D D^T = \bar{L} \bar{L}^T$, then it is shown that $\tilde{r} = \|\bar{L}^{-1} B\| r + \|\bar{L}^{-1} D\| q \leq 2$ and that

$|\det \bar{L}| \leq |\det \tilde{L}| (\|\tilde{L}^{-1} B\| r + \|\tilde{L}^{-1} D\| q)^n$ for any non-singular \tilde{L} , that is, that this choice of \bar{L} provides an ellipsoid enclosure that is optimal to within a factor of 2 of the radius (note that $|\det \tilde{L}| (\|\tilde{L}^{-1} B\| r + \|\tilde{L}^{-1} D\| q)^n$ is an upper bound to the volume of the

ellipsoid for the arbitrarily chosen \tilde{L}). However, it is also noted that the optimality of the radius chosen is subject to that of the bound $\tilde{r} \leq \|\tilde{L}^{-1}B\|r + \|\tilde{L}^{-1}D\|q$.

The choice of \tilde{L} and D still remains non-uniquely determined, and for reasons of computational stability, \tilde{L} is obtained as a Cholesky factor of $r^2BB^T + q^2DD^T$ and $D = \text{diag}\{d_i + d'_i r\}$.

In summary, this procedure provides an ellipsoidal enclosure for the image-set of the points belonging to an initial ellipsoid by an interval affine transformation. In practice, to use this method for propagating the state vector of a dynamic system given an initial interval vector, which is representable by an n dimensional hyper rectangle, or box, an ellipsoidal enclosure to this initial state is first calculated. Although the ellipsoid circumscribing a given box is not unique, one option is to choose the minimal volume circumscribing ellipsoid, and is the method adopted in the subsequent examples.

Consider the simulation of the interval system (10) and (11), with A^I , B^I , & C^I given by (21) to (23), where the nominal values of the interval matrices are the ones specified in (3), using the same inputs $u(k)$ used in the previous simulation, and with an initial interval-valued state vector given by

$$x(0) = \begin{bmatrix} [-0.005, 0.005] \\ [-0.005, 0.005] \end{bmatrix} \quad (26)$$

Figure 5(a) depicts the propagation of the state intervals using (rectangular) IA, whereas Figure 5(b) shows the same calculations but using ellipsoidal arithmetic with Neumaier's enclosures. Clearly the elliptical enclosures are far tighter than the corresponding rectangular ones. Note that the interval affine transformation of the interval state vector at each time-step is given by (10), in which A^I represents a linear interval transformation (i.e., set of linear transformations), and $b^I(k) \stackrel{\text{def}}{=} B^I u(k) + \omega(k)$ an interval translation vector (i.e. set of translations). The eigenvalues of the

nominal linear transformation, A , are the complex conjugate pair $0.4 \pm 0.25i$, so the system is somewhat underdamped.

Now consider the simulation of an interval system with nominal overdamped dynamics given by

$$A = \begin{bmatrix} 0.6 & -0.05 \\ 1 & 0 \end{bmatrix}, B = \begin{bmatrix} 1 \\ 0 \end{bmatrix}, C = [0 \quad 1] \quad (27)$$

and interval matrices centred around these nominal ones with interval widths of 5% on either side, as stated in (21) to (23). As before, simulation is carried out for one-hundred time-steps, with a reference target y_r being set at 20, 50 and -15 for each one-third of the simulation respectively, and a state-feedback control law as in (9) with $K_c = [-0.1, 0.01]$ and $K_s = 0.8$ calculated to have the same closed-loop poles as before (0.6 and 0.1) (note that for generating the control input, the true state of the system is used, as the main concern here is not the control law generated but the calculation of the interval state trajectory). The resulting state propagation using (rectangular) IA and ellipsoidal arithmetic are shown in Figures 6(a) and 6(b) respectively, with the initial state being described by (26). In this case, IA provides tighter bounds to the state-vector sets than does ellipsoidal arithmetic. It is interesting to note that in this case, the nominal poles of the system are at 0.5 and 0.1.

The tightness of the ellipsoidal enclosures computed according to Neumaier's algorithm depends on the nature of the linear interval transformation matrix A^I . If the eigenvalues are predominantly complex conjugate (corresponding to underdamped systems), then the transformation has a greater rotation component, and Neumaier's enclosures work well. On the other hand, for real eigenvalues (corresponding to overdamped systems), the transformation has a larger shear component, and the

ellipsoid enclosures become very elongated in the direction of largest stretching. Thus it becomes a necessity to develop a method that can be of use in either situation.

In order to provide enclosures that are tight for both under and overdamped systems, the following algorithm is proposed for recursive affine transformations. Given an initial interval vector, which is an n -dimensional box, B_0 , obtain the smallest ellipsoid containing it, E_0 . The word “smallest” is used here vaguely, but one option (and the one implemented here) is to choose the ellipsoid with the smallest volume that contains the box, that is, an ellipsoid with the same eccentricity as the box. Then proceed to apply the interval affine transformation to both enclosures, B_0 via (rectangular) IA and E_0 via ellipsoidal arithmetic, resulting in B_1 and E_1 , respectively. Note that the tightest set containing the transformed points at this stage will be given by the intersection of B_1 and E_1 , which however is in general neither a box nor an ellipsoid. Thus, obtain the tightest box B_2 that contains E_1 , which, intersected with B_1 results in B_3 . The box B_3 is now the smallest box-enclosure that contains the transformed set, and is used as the starting box for the next interval transformation. On the other hand, obtain E_3 as the smallest ellipsoid containing B_3 . Then select the smaller of E_1 and E_3 as the starting ellipsoid to be transformed by the next interval affine transformation. Again, smaller in this case could be in terms of volume, sum of semi-axes, etc. The algorithm is summarised in Figure 7.

5. The IKF equations as affine transformations

The ellipsoidal arithmetic approach is possible because ellipsoids are invariant under affine transformations. In order to be able to apply ellipsoidal arithmetic to the IKF equations, these must first be expressed as recursive affine transformations. The IKF equations were given in (16) to (20) and can be divided into three sets: propagation of

the state-vector, propagation of the error covariance, and calculation of the Kalman gain.

With respect to propagation of the state vector, (16) and (19) must be applied in turn. The prediction equation (16) is already in the form of an interval affine transformation, whereas (19) can be written as

$$\hat{x}^I(k|k) = \{ I - K^I(k) C^I \} \hat{x}^I(k|k-1) + K^I(k) y(k) \quad (28)$$

which, if $K^I(k)$ has already been obtained, is also clearly an interval affine transformation.

For the error covariance estimates, consider the prediction equation (17) written using indicial notation:

$$p_{i,j}^I(k|k-1) = a_{i,l}^I a_{j,m}^I p_{l,m}^I(k-1|k-1) + q_{i,j}; \quad i, j, l, m = 1, \dots, n \quad (29)$$

In order to represent the state estimate error and disturbance covariance matrices as vectors, consider $\tilde{p}^I(k|k-1)$, $\tilde{p}^I(k-1|k-1)$, and $\tilde{q} \in \mathbb{R}^{n^2}$ defined as:

$$\tilde{p}_{n(i-1)+j}^I(k|k-1) \stackrel{\text{def}}{=} p_{i,j}^I(k|k-1), \quad i, j = 1, \dots, n \quad (30)$$

$$\tilde{p}_{n(i-1)+j}^I(k-1|k-1) \stackrel{\text{def}}{=} p_{i,j}^I(k-1|k-1), \quad i, j = 1, \dots, n \quad (31)$$

$$\tilde{q}_{n(i-1)+j} \stackrel{\text{def}}{=} q_{i,j}, \quad i, j = 1, \dots, n \quad (32)$$

Then by (29), the relationship between these is

$$\begin{aligned} \tilde{p}_{n(i-1)+j}^I(k|k-1) &= p_{i,j}^I(k|k-1) = a_{i,l}^I a_{j,m}^I p_{l,m}^I(k-1|k-1) + q_{i,j} = \\ &a_{i,l}^I a_{j,m}^I \tilde{p}_{n(l-1)+m}^I(k-1|k-1) + \tilde{q}_{n(i-1)+j} \end{aligned} \quad (33)$$

which is an interval affine transformation of the vector $\tilde{p}_{n(l-1)+m}^I(k-1|k-1)$. To see

this, define

$$(\tilde{a}_{i,j}^I) \in \Re^{n^2 \times n^2} : \tilde{a}_{n(i-1)+j, n(l-1)+m}^I \stackrel{\text{def}}{=} a_{i,l}^I a_{j,m}^I, \quad i, j, l, m = 1, \dots, n \quad (34)$$

and also

$$r \stackrel{\text{def}}{=} n(i-1) + j, \quad s \stackrel{\text{def}}{=} n(l-1) + m \quad (35)$$

from which

$$j = r - n(i-1), \quad m = s - n(l-1) \quad (36)$$

Thus,

$$\tilde{a}_{r,s}^I = a_{i,l}^I a_{r-n(i-1), s-n(l-1)}^I \quad \text{for } i, l \in \{1, \dots, n\} \text{ \& } r - n(i-1), s - n(l-1) \in \{1, \dots, n\} \quad (37)$$

that is,

$$\tilde{a}_{r,s}^I = a_{i,l}^I a_{r-n(i-1), s-n(l-1)}^I \quad \text{for } i, l \in \{1, \dots, n\}, \quad r \in \{1 + n(i-1), 2 + n(i-1), \dots, n + n(i-1)\}, \quad s \in \{1 + n(l-1), 2 + n(l-1), \dots, n + n(l-1)\} \quad (38)$$

With these definitions, (33) is expressed as:

$$\tilde{p}_r^I(k|k-1) = \tilde{a}_{r,s}^I \tilde{p}_s^I(k-1|k-1) + \tilde{q}_r; \quad r, s = 1, \dots, n^2 \quad (39)$$

which is clearly seen to be an interval affine transformation of $\tilde{p}_s^I(k-1|k-1)$.

Similarly, the correction equation (20) in indicial notation is

$$p_{i,j}^I(k|k) = \{I - K^I(k) C^I\}_{i,l} p_{l,j}^I(k|k-1), \quad i, j, l = 1, \dots, n \quad (40)$$

As before, define

$$\tilde{p}^I(k|k) \in \mathfrak{R}^{n^2} : \tilde{p}_{n(i-1)+j}^I(k|k) \stackrel{\text{def}}{=} p_{i,j}^I(k|k), \quad i, j = 1, \dots, n \quad (41)$$

and with $\tilde{p}^I(k|k-1)$ defined as before, (40) can be written as

$$\begin{aligned} \tilde{p}_{n(i-1)+j}^I(k|k) &= p_{i,j}^I(k|k) = \{I - K^I(k) C^I\}_{i,l} p_{i,j}^I(k|k-1) = \\ &\{I - K^I(k) C^I\}_{i,l} \tilde{p}_{n(l-1)+j}^I(k|k-1) \end{aligned} \quad (42)$$

which specifies an interval affine transformation of the vector $\tilde{p}_{n(l-1)+j}^I(k|k-1)$. Once again, this can be seen more clearly by defining

$$\begin{aligned} (\tilde{h}_{i,j}^I) \in \mathfrak{R}^{n^2 \times n^2} : \tilde{h}_{n(i-1)+j, n(l-1)+j}^I &\stackrel{\text{def}}{=} \begin{cases} \{I - K^I(k) C^I\}_{i,l} & \text{for } i, l = 1, \dots, n \\ 0 & \text{otherwise} \end{cases}, j = \\ 1, \dots, n \end{aligned} \quad (43)$$

and also

$$r \stackrel{\text{def}}{=} n(i-1) + j, \quad s \stackrel{\text{def}}{=} n(l-1) + j \quad (44)$$

from which

$$i = \frac{r-j}{2} + 1, \quad l = \frac{s-j}{2} + 1 \quad (45)$$

Thus,

$$\begin{aligned} \tilde{h}_{r,s}^I &\stackrel{\text{def}}{=} \begin{cases} \{I - K^I(k) C^I\}_{\frac{r-j}{2}+1, \frac{s-j}{2}+1} & \text{if } \frac{r-j}{2} + 1, \frac{s-j}{2} + 1 \in \{1, \dots, n\} \\ 0 & \text{otherwise} \end{cases}, j = 1, \dots, n; r, s = \\ 1, \dots, n^2 \end{aligned} \quad (46)$$

ie,

$$\tilde{h}_{r,s}^I \stackrel{\text{def}}{=} \begin{cases} \{I - K^I(k) C^I\}_{\frac{r-j}{2}+1, \frac{s-j}{2}+1} & \text{if } r, s \in \{j, j+2, \dots, j+n(n-1)\} \\ 0 & \text{otherwise} \end{cases}, j = 1, \dots, n; r, s = 1, \dots, n^2 \quad (47)$$

Then, (42) can be written as

$$\tilde{p}_r^I(k|k) = \tilde{h}_{r,s}^I \tilde{p}_s^I(k|k-1); r, s = 1, \dots, n^2 \quad (48)$$

which is clearly in the form of an affine transformation.

For example, for $n = 2$, the error covariance prediction equation is

$$\begin{bmatrix} p_{1,1}^I(k|k-1) & p_{1,2}^I(k|k-1) \\ p_{2,1}^I(k|k-1) & p_{2,2}^I(k|k-1) \end{bmatrix} = \begin{bmatrix} a_{1,1}^I & a_{1,2}^I \\ a_{2,1}^I & a_{2,2}^I \end{bmatrix} \begin{bmatrix} p_{1,1}^I(k-1|k-1) & p_{1,2}^I(k-1|k-1) \\ p_{2,1}^I(k-1|k-1) & p_{2,2}^I(k-1|k-1) \end{bmatrix} \begin{bmatrix} a_{1,1}^I & a_{2,1}^I \\ a_{1,2}^I & a_{2,2}^I \end{bmatrix} + \begin{bmatrix} q_{1,1} & q_{1,2} \\ q_{2,1} & q_{2,2} \end{bmatrix} \quad (49)$$

which can be expressed as

$$\begin{bmatrix} \tilde{p}_1^I(k|k-1) \\ \tilde{p}_2^I(k|k-1) \\ \tilde{p}_3^I(k|k-1) \\ \tilde{p}_4^I(k|k-1) \end{bmatrix} = \begin{bmatrix} a_{1,1}^I & a_{1,1}^I & a_{1,1}^I a_{1,2}^I & a_{1,2}^I a_{1,1}^I & a_{1,2}^I a_{1,2}^I \\ a_{1,1}^I a_{2,1}^I & a_{1,1}^I a_{2,2}^I & a_{1,2}^I a_{2,1}^I & a_{1,2}^I a_{2,2}^I \\ a_{2,1}^I a_{1,1}^I & a_{2,1}^I a_{1,2}^I & a_{2,2}^I a_{1,1}^I & a_{2,2}^I a_{1,2}^I \\ a_{2,1}^I a_{2,1}^I & a_{2,1}^I a_{2,2}^I & a_{2,2}^I a_{2,1}^I & a_{2,2}^I a_{2,2}^I \end{bmatrix} \begin{bmatrix} \tilde{p}_1^I(k-1|k-1) \\ \tilde{p}_2^I(k-1|k-1) \\ \tilde{p}_3^I(k-1|k-1) \\ \tilde{p}_4^I(k-1|k-1) \end{bmatrix} + \begin{bmatrix} \tilde{q}_1 \\ \tilde{q}_2 \\ \tilde{q}_3 \\ \tilde{q}_4 \end{bmatrix} \quad (50)$$

where

$$\begin{bmatrix} \tilde{p}_1^I(k|k-1) \\ \tilde{p}_2^I(k|k-1) \\ \tilde{p}_3^I(k|k-1) \\ \tilde{p}_4^I(k|k-1) \end{bmatrix} \stackrel{\text{def}}{=} \begin{bmatrix} p_{1,1}^I(k|k-1) \\ p_{1,2}^I(k|k-1) \\ p_{2,1}^I(k|k-1) \\ p_{2,2}^I(k|k-1) \end{bmatrix},$$

$$\begin{bmatrix} \tilde{p}_1^I(k-1|k-1) \\ \tilde{p}_2^I(k-1|k-1) \\ \tilde{p}_3^I(k-1|k-1) \\ \tilde{p}_4^I(k-1|k-1) \end{bmatrix} \stackrel{\text{def}}{=} \begin{bmatrix} p_{1,1}^I(k-1|k-1) \\ p_{1,2}^I(k-1|k-1) \\ p_{2,1}^I(k-1|k-1) \\ p_{2,2}^I(k-1|k-1) \end{bmatrix} \& \begin{bmatrix} \tilde{q}_1 \\ \tilde{q}_2 \\ \tilde{q}_3 \\ \tilde{q}_4 \end{bmatrix} \stackrel{\text{def}}{=} \begin{bmatrix} q_{1,1} \\ q_{1,2} \\ q_{2,1} \\ q_{2,2} \end{bmatrix} \quad (51)$$

Similarly, the error covariance correction equation is

$$\begin{bmatrix} p_{1,1}^I(k|k) & p_{1,2}^I(k|k) \\ p_{2,1}^I(k|k) & p_{2,2}^I(k|k) \end{bmatrix} = \begin{bmatrix} h_{1,1}^I & h_{1,2}^I \\ h_{2,1}^I & h_{2,2}^I \end{bmatrix} \begin{bmatrix} p_{1,1}^I(k|k-1) & p_{1,2}^I(k|k-1) \\ p_{2,1}^I(k|k-1) & p_{2,2}^I(k|k-1) \end{bmatrix} \quad (52)$$

which is equivalent to

$$\begin{bmatrix} \tilde{p}_1^I(k|k) \\ \tilde{p}_2^I(k|k) \\ \tilde{p}_3^I(k|k) \\ \tilde{p}_4^I(k|k) \end{bmatrix} = \begin{bmatrix} h_{1,1}^I & 0 & h_{1,2}^I & 0 \\ 0 & h_{1,1}^I & 0 & h_{1,2}^I \\ h_{2,1}^I & 0 & h_{2,2}^I & 0 \\ 0 & h_{2,1}^I & 0 & h_{2,2}^I \end{bmatrix} \begin{bmatrix} \tilde{p}_1^I(k|k-1) \\ \tilde{p}_2^I(k|k-1) \\ \tilde{p}_3^I(k|k-1) \\ \tilde{p}_4^I(k|k-1) \end{bmatrix} \quad (53)$$

if

$$\begin{bmatrix} \tilde{p}_1^I(k|k) \\ \tilde{p}_2^I(k|k) \\ \tilde{p}_3^I(k|k) \\ \tilde{p}_4^I(k|k) \end{bmatrix} \stackrel{\text{def}}{=} \begin{bmatrix} p_{1,1}^I(k|k) \\ p_{1,2}^I(k|k) \\ p_{2,1}^I(k|k) \\ p_{2,2}^I(k|k) \end{bmatrix} \quad (54)$$

Finally, the Kalman gain is updated as a rectangular enclosure at each step according to (18) directly using IA.

6. Interval Kalman filtering using the hybrid ellipsoidal-rectangular enclosure algorithm

Consider again the simulation of the two interval systems of the preceding section, namely, the systems described by (10) and (11), with A^I , B^I , & C^I given by (21) to (23), and nominal values of the interval matrices given, in the first case, by (3) (underdamped nominal dynamics), and in the second, by (27) (overdamped nominal dynamics). For each case, using the same inputs $u(k)$ used in the preceding section, and the same disturbance and noise processes described earlier, the state-trajectory and output of the nominal system are simulated from an initial state situated at the origin of the state-space. Also, based on the initial estimates given in (24), the IKF equations are in turn simulated using purely IA based computations, via the ellipsoidal arithmetic recursions described in the preceding section, and lastly using the hybrid ellipsoidal-rectangular enclosure algorithm. The resulting state enclosures at each time step are depicted in Figures 8 to 11.

As seen from the figures, in the case of the underdamped system with complex conjugate poles, the rectangular enclosures obtained via IA overestimate the actual state sets to such an extent that simulation cannot continue after a certain point, whereas the ellipsoidal arithmetic IKF provides much tighter bounds. The hybrid enclosure IKF in this case offers bounds similar to those of the ellipsoidal arithmetic IKF. In the case of the overdamped system with real poles, however, it is the rectangular IA IKF enclosures that provide the tighter bounds to the sets of state vectors, and so the hybrid enclosure IKF relies mostly on these.

7. Conclusions

For systems with bounded modelling uncertainty, the IKF provides guaranteed bounds to the optimal estimate of the state vector. Even if the exact values of the states

are not known, guaranteed bounds to these can be useful, for example, to ensure that they remain within some desirable or permissible operating region. However, implementation of the IKF via IA can result in over conservative bounds which are not representative of the actual set of possible optimal states, and in some cases can even grow indefinitely. It thus becomes necessary to develop alternative methods by which to compute the IKF estimates which yield stable and tighter bounds.

The case studies presented in this paper show that implementation of the IKF equations by means of the hybrid enclosure algorithm provides stable and tighter bounds for a wider range of system dynamic characteristics than does the direct application of IA which generates rectangular enclosures. The hybrid enclosure approach is based on using ellipsoidal arithmetic as well as IA to propagate both an ellipsoidal and rectangular enclosure of the state vector at each time step, respectively, and subsequently fusing these prior to the next iteration. These fusions only require the intersecting of boxes and circumscribing these by ellipsoids, and are computationally inexpensive.

Although it was shown that for certain types of systems the rectangular IA enclosures consistently provide tighter bounds than the ellipsoidal arithmetic ellipsoids, and that for another class of systems the opposite occurs, the advantage of using the hybrid enclosure approach over one or other set arithmetic is that for borderline cases the more effective type of enclosure may alternate from iteration to iteration. Moreover, in practice the dynamics of a system can be prone to large scale variations. Control strategies for such systems are often based on multiple model representations of the same. Thus, even though the large scale dynamical changes in the nominal model of the system may be known, it is necessary to use an IKF implementation that is effective for a broad spectrum of possible dynamic characteristics.

Furthermore, it should also be noted that if the closed-loop dynamics of the system are specified, such as in the examples shown here, then the IKF may be defined directly upon the resulting closed loop interval model obtained from applying the feedback control law to the uncertain open-loop model. The IKF implementation must therefore be robust to the choice of desired closed-loop specifications, or changes to these specifications over time.

For the aforementioned reasons, the use of the hybrid enclosure implementation is clearly advantageous. Its mathematical development has been presented for generic linear state space models of any order, and its application will enable the practical and efficient use of the IKF as a guaranteed state estimator for all kinds of systems with bounded parametric uncertainty that respond to the linear model. Suggested future research includes further sharpening of the interval bounds by incorporating the calculation of an enclosure to the Kalman gain into the recursive ellipsoidal arithmetic scheme, or finding an alternative arithmetic that can implement all of the IKF equations. Another useful development would be the extension of the method to the nonlinear case (interval extended KF).

Nomenclature

KF	Kalman filter
IKF	Interval Kalman filter
INTLAB	Interval laboratory
IA	Interval arithmetic
$A(A^I)$	real (interval) valued state transition matrix / linear transformation matrix

$B(B^I)$	real (interval) valued input matrix
$C(C^I)$	real (interval) valued output matrix
$E(z, L, r)$	set of points $\{z + L \xi : \xi \in \mathbb{R}^n, \ \xi\ \leq r\}$, $z \in \mathbb{R}^n, L \in \mathbb{R}^{n \times n}, r \in \mathbb{R}_+$
$K(K^I)$	real (interval) valued Kalman gain
K_c	state feedback gain vector
K_s	scaling gain
I	identity matrix
$I\mathbb{R}$	set of nonempty, closed and bounded real intervals
N	normal distribution
$P(P^I)$	real (interval) valued error covariance matrix
Q	input disturbance covariance matrix
R	output noise covariance matrix
$\mathbb{R}(\mathbb{R}_+)$	set of real (positive real) numbers
$a^I(\tilde{a}^I)$	interval valued (augmented) state transition matrix
$b(b^I)$	linear (linear interval) translation vector
\tilde{h}^I	interval valued error covariance transition matrix
k	iteration number
$m_{i,j}$	(i,j)th element of m
$p^I(\tilde{p}^I)$	interval valued error covariance matrix (vector)
$q^I(\tilde{q}^I)$	interval valued input disturbance covariance matrix (vector)
u	input or control vector
x	real state vector
$\hat{x}(\hat{x}^I)$	real (interval) state vector estimate
y	output vector
y_r	reference output

$ \cdot $	element wise absolute value
$\ \cdot\ $	Euclidean norm
$:=$	assignment operator
Δ	increment
α	angular value
v	output noise vector / Frobenius norm
ω	disturbance input vector

References

- Ahn, H., Kim, Y., & Chen, Y. (2012). An interval Kalman filtering with minimal conservatism. *Applied Mathematics and Computation*, 218(18), 9563-9570.
- Bertsekas, D., & Rhodes, I. (1971). Recursive state estimation for a set-membership description of uncertainty. *IEEE Transactions on Automatic Control*, 16(2), 117-128.
- Chen, G., Wang, J., & Shieh, L. S. (1997). Interval Kalman Filtering. *IEEE Transactions on Aerospace and Electronic Systems*, 33(1), 250–258.
- Gao, H., & Chen, T. (2007). H-Infinity estimation for uncertain systems with limited communication capacity. *IEEE Trans. on Automatic Control*, 5(11), 2070-2084.
- He, X. F., and Vik, B. (1999). Use of Extended Interval Kalman Filter on Integrated GPS/INS System. *Proceedings of the 12th International Technical Meeting of the Satellite Division of The Institute of Navigation*, (pp. 1907-1914). Nashville, TN.
- Jain, B. N. (1975). Guaranteed error estimation in uncertain systems. *IEEE Transactions on Automatic Control*, 20(2), 230-232.
- Jaulin, L. (2009). Robust set membership state estimation. Application to Underwater Robotics. *Automatica*, 45(1), 202-206.
- Julier, S., & Uhlmann, J. (1997). A new extension of the Kalman filter to nonlinear systems. *Proc. of AeroSense: The 11th Int. Symp. on Aerospace/Defense Sensing, Simulations and Controls* (pp. 182-193). Orlando, FL, USA.
- Kalman, R. E. (1960). A New Approach to Linear Filtering and Prediction Problems. *Transactions of the ASME, Journal of Basic Engineering*, 82, 35-45.

- Moore, R. E. (1966). *Interval Analysis*. Prentice-Hall, Englewood, NJ.
- Motwani, A., Sharma, S. K., Sutton, R., & Culverhouse, P. (2013). Interval Kalman Filtering in Navigation System Design for an Uninhabited Surface Vehicle. *Journal of Navigation*, 66, 639-652.
- Neumaier, A. (1993). The wrapping effect, ellipsoid arithmetic, stability and confidence regions. *Computing Supplementum*, 9, 175-190.
- Petersen, I. R., & McFarlane, D. C. (1996). Optimal guaranteed cost filtering for uncertain discrete-time linear systems. *Int. J. Robust Nonlinear Control*, 6, 267–280.
- Rump, S. (1999). *INTLAB - INTerval LABoratory*. Kluwer Academic Publishers.
- Savkin, A. V., & Petersen, I. R. (1998). Robust state estimation and model validation for discrete-time uncertain systems with a deterministic description of noise and uncertainty. *Automatica*, 34(2), 271-274.
- Sayed, A. H. (2001). A framework for state-space estimation with uncertain models. *IEEE Trans Autom Control*, 47, 998–1013.
- Siouris, G., Chen, G. and Wang, J. (1997). Tracking an Incoming Ballistic Missile using an Extended Interval Kalman filter. *IEEE Transactions on Aerospace and Electronic Systems*, 33(1), 232–240.
- Smith, G. A., Schmidt, S. F., & McGee, L. A. (1961). Application of statistical filter theory to the optimal estimation of position and velocity on board a circumlunar vehicle (Technical Report R-35). Moffett Federal Airfield, CA.
- Tiano, A., Zirilli, A., Cuneo, M. and Pagnan, S. (2005). Multisensor Data Fusion Applied to Marine Integrated Navigation Systems. *Proceedings of the IMechE Part M: Journal of Engineering for the Maritime Environment*, 219(3), 121-130.
- Tiano, A., Zirilli, A., & Pizzocchero, F. (2001). Application of interval and fuzzy techniques to integrated navigation systems. *Joint 9th IFSA World Congress and 20th NAFIPS International Conference proceedings*, 1 (pp.13-18). Vancouver, British Columbia, Canada.
- Weng, Z., Chen, G., Shieh, L. S., & Larsson, J. (2000). Evolutionary Programming Kalman Filter. *Information Sciences*, 129, 197–210.
- Wu, H., and Chen, G. (1999). Suboptimal Kalman filtering for linear systems with Gaussian-sum type of noise. *Mathematical and Computer Modelling*, 29(3), 101-125.

Zhu, Y. (2012). From Kalman filtering to set-valued filtering for dynamic systems with uncertainty. *Communications in Information and Systems*, 12(1), 97-130.

Accepted Manuscript

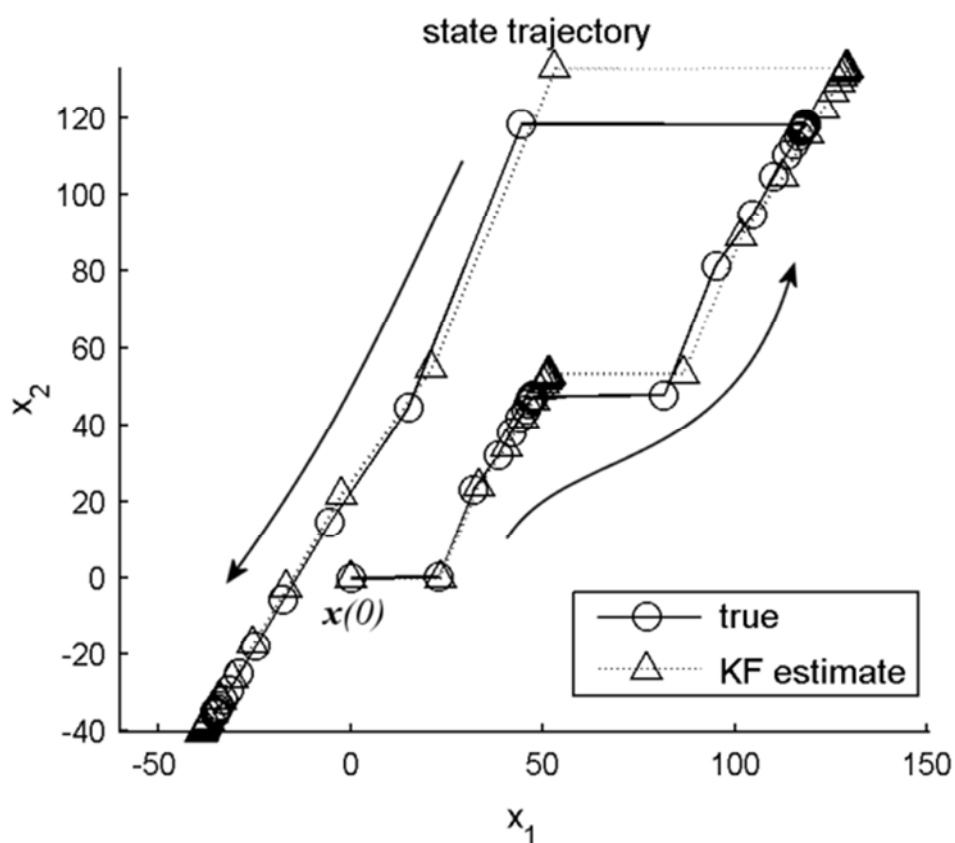


Figure 1. State trajectory and KF state trajectory estimate.

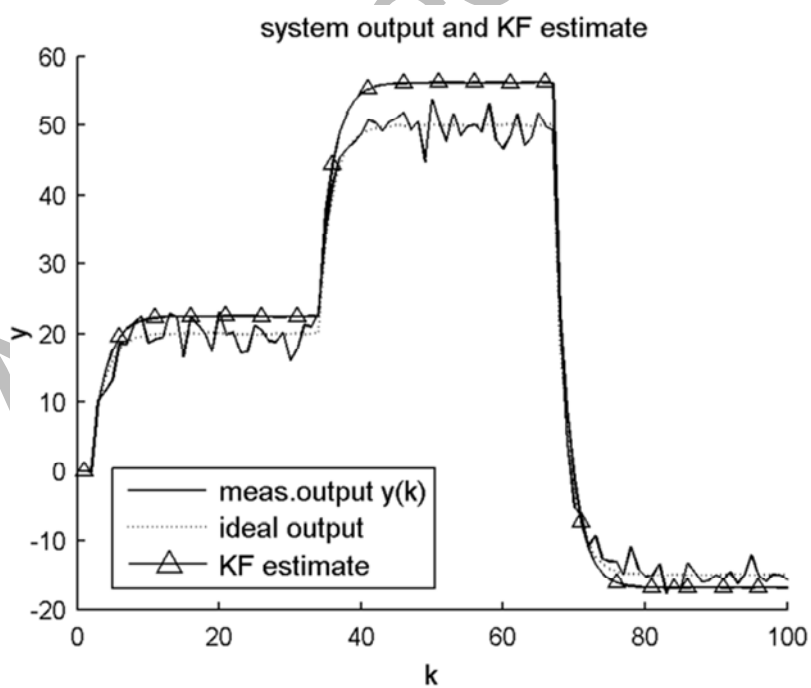


Figure 2. System output $y(k)$, noise-less output $Cx(k)$, and KF output estimate.

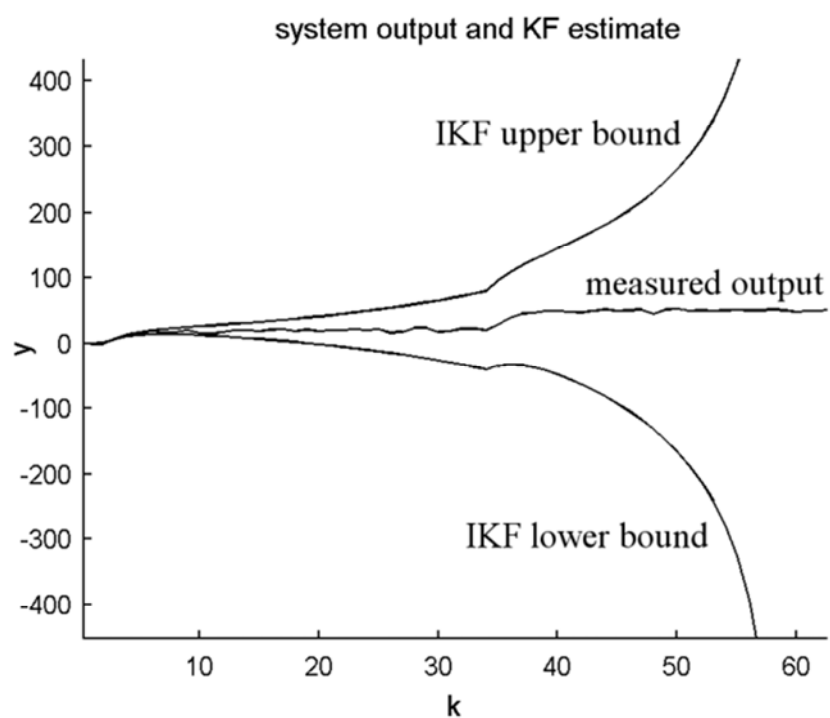


Figure 3. System output $y(k)$ and IKF interval-estimate thereof.

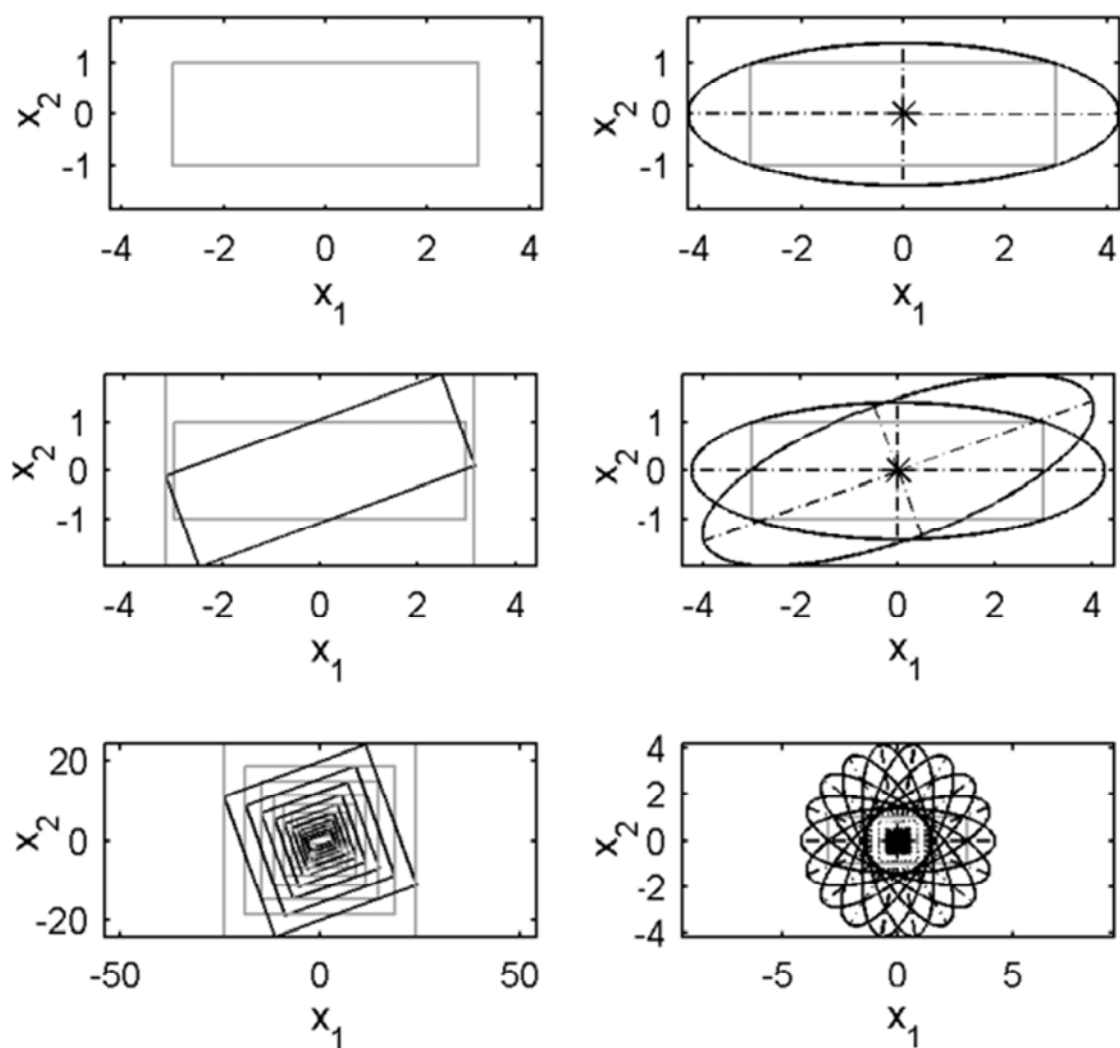


Figure 4. Comparison of successive rotations of a 2D interval vector using (rectangular) IA and using elliptical arithmetic.

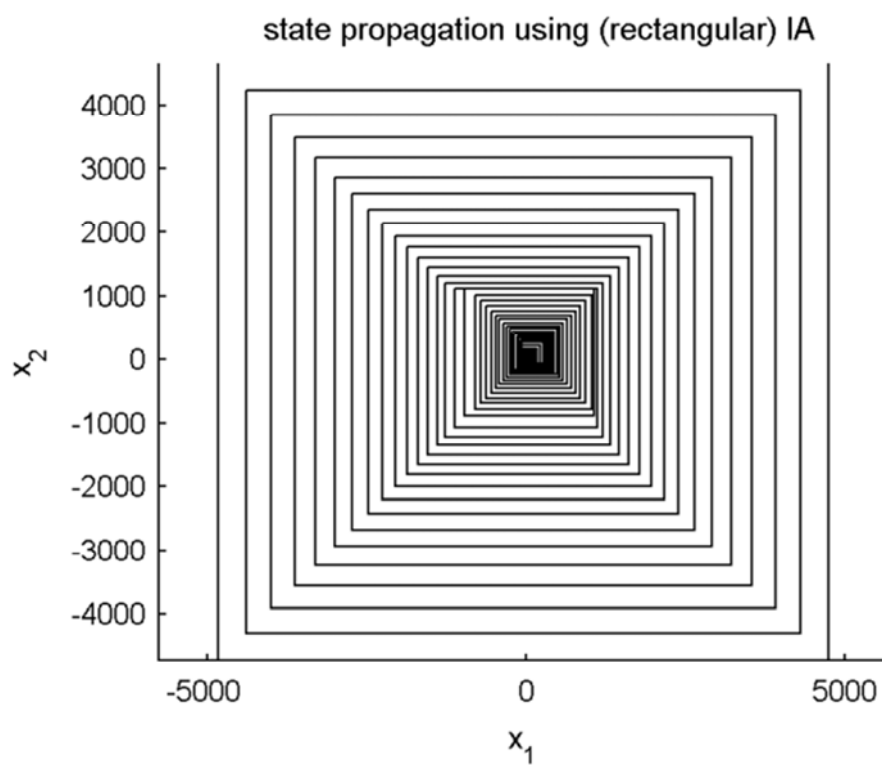


Figure 5(a). Simulation of the state-vector for the interval system with nominal poles at $0.4 \pm 0.25i$ using IA.

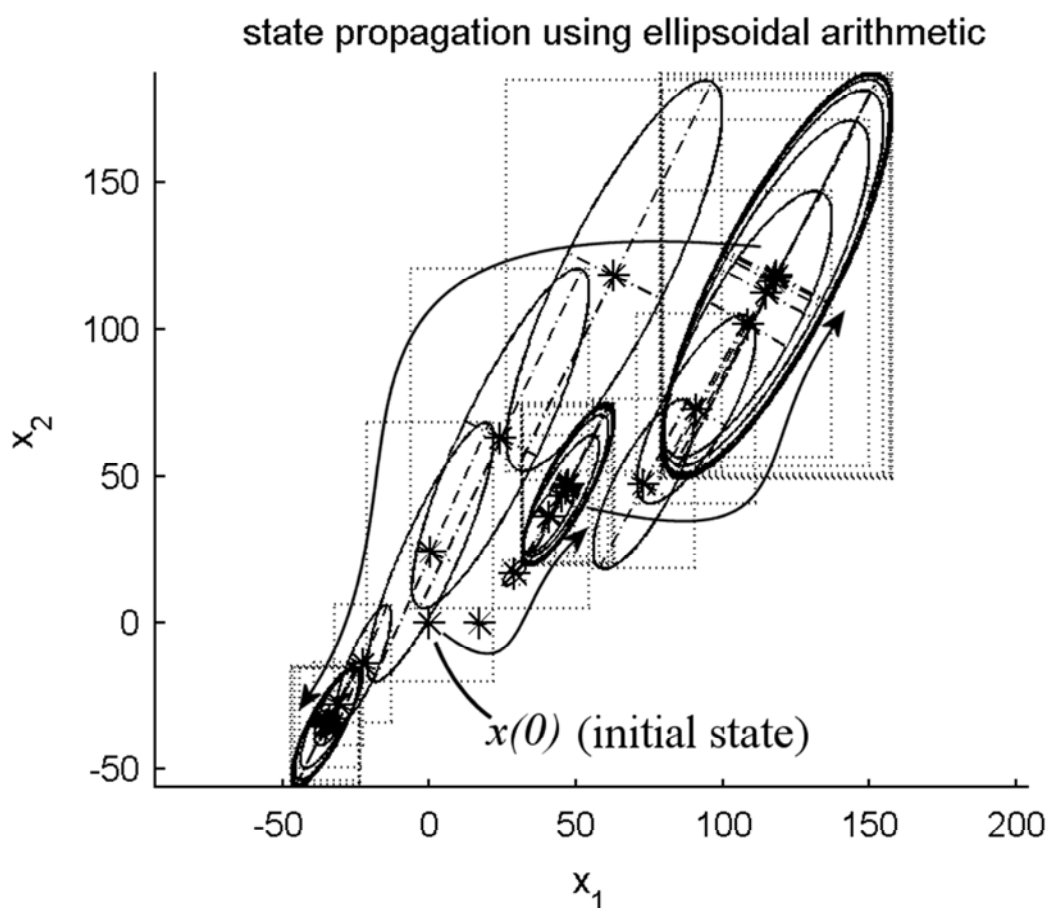


Figure 5(b). Simulation of the state-vector for the interval system with nominal poles at $0.4 \pm 0.25i$ using ellipsoidal arithmetic.

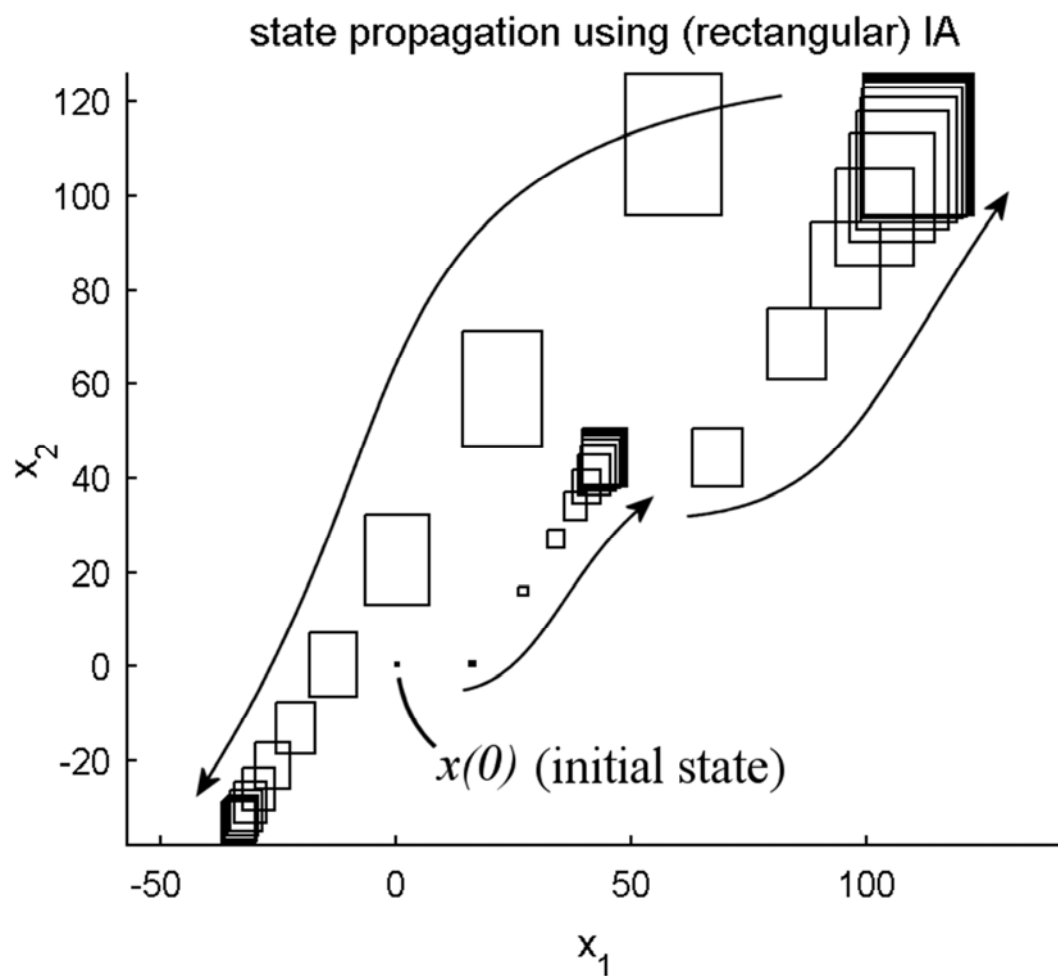


Figure 6(a). Simulation of the state-vector for the interval system with nominal poles at 0.5 and 0.1 using IA.

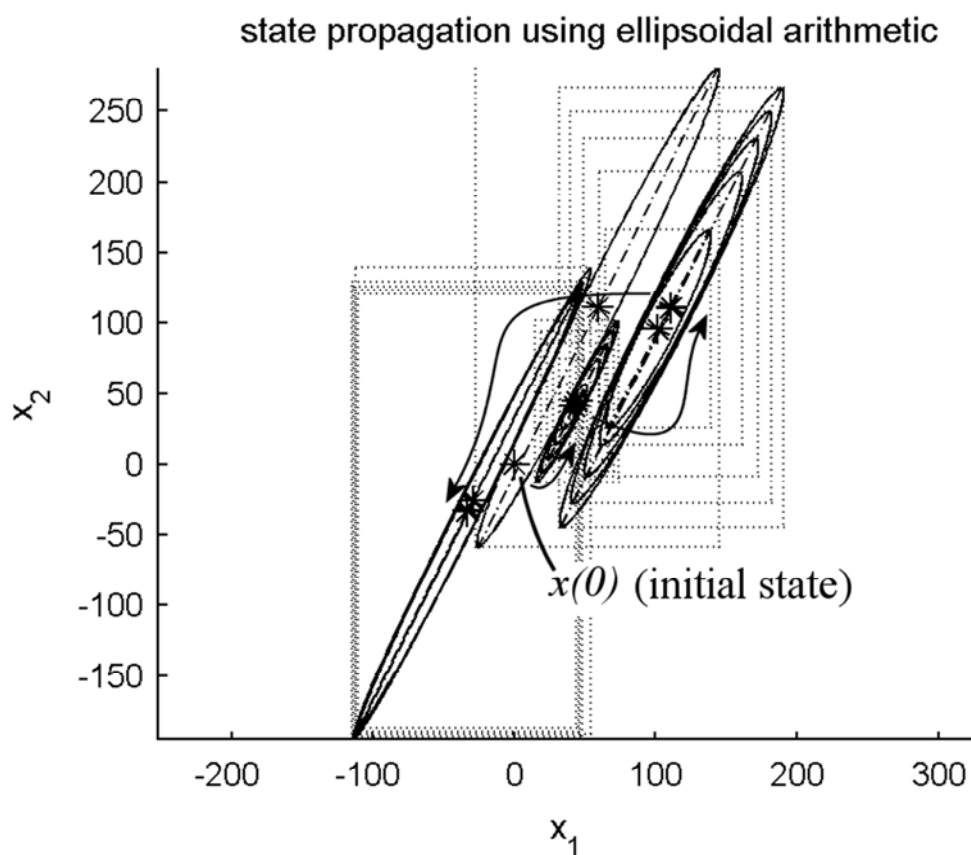


Figure 6(b). Simulation of the state-vector for the interval system with nominal poles at 0.5 and 0.1 using ellipsoidal arithmetic.

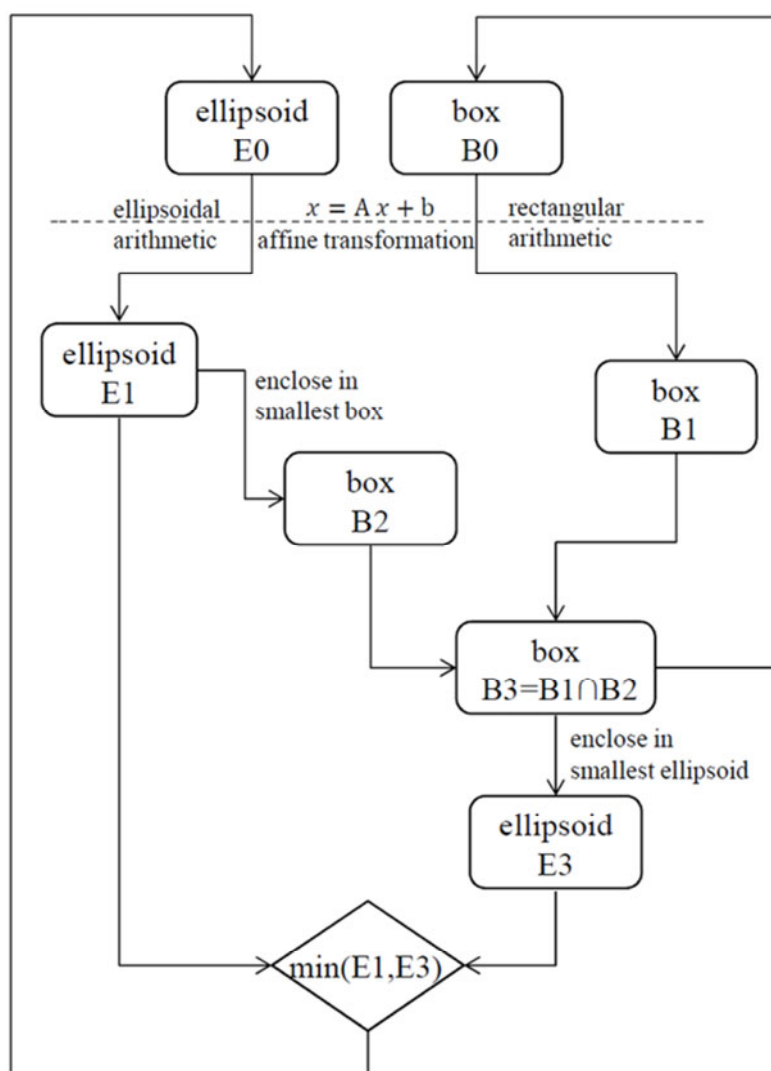


Figure 7. The hybrid ellipsoidal-rectangular enclosure algorithm.

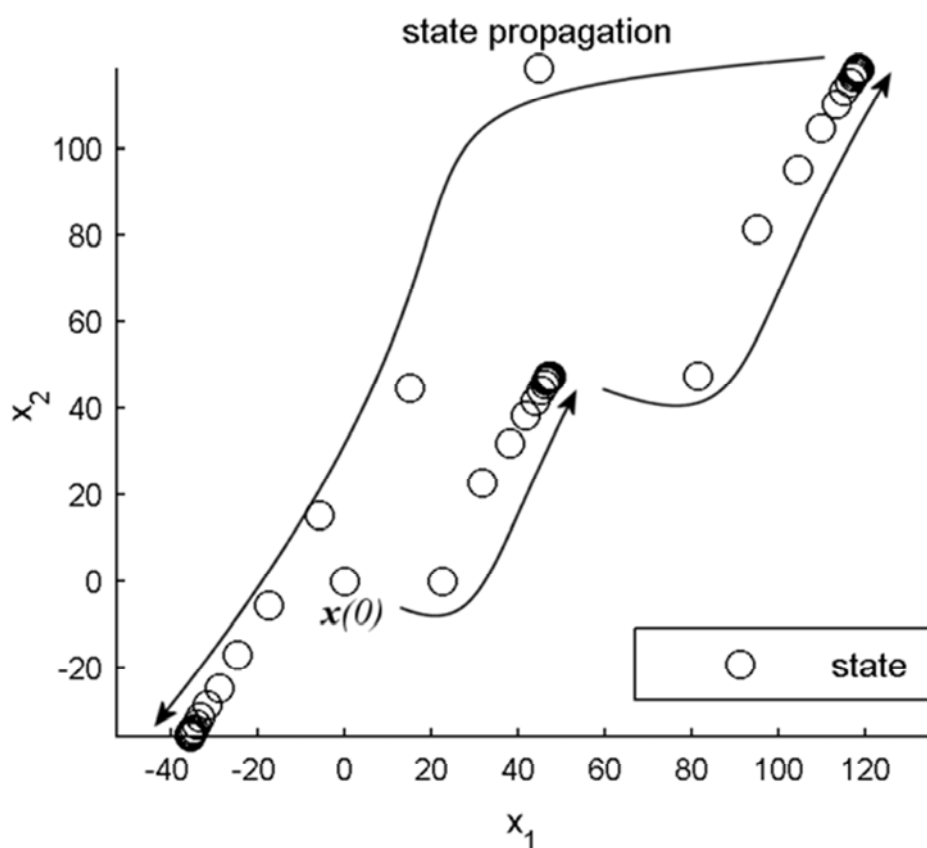


Figure 8(a). Simulation of the state-vector for the nominal underdamped system with poles at $0.4 \pm 0.25i$. States are depicted as circles for clarity, although they represent point-values.

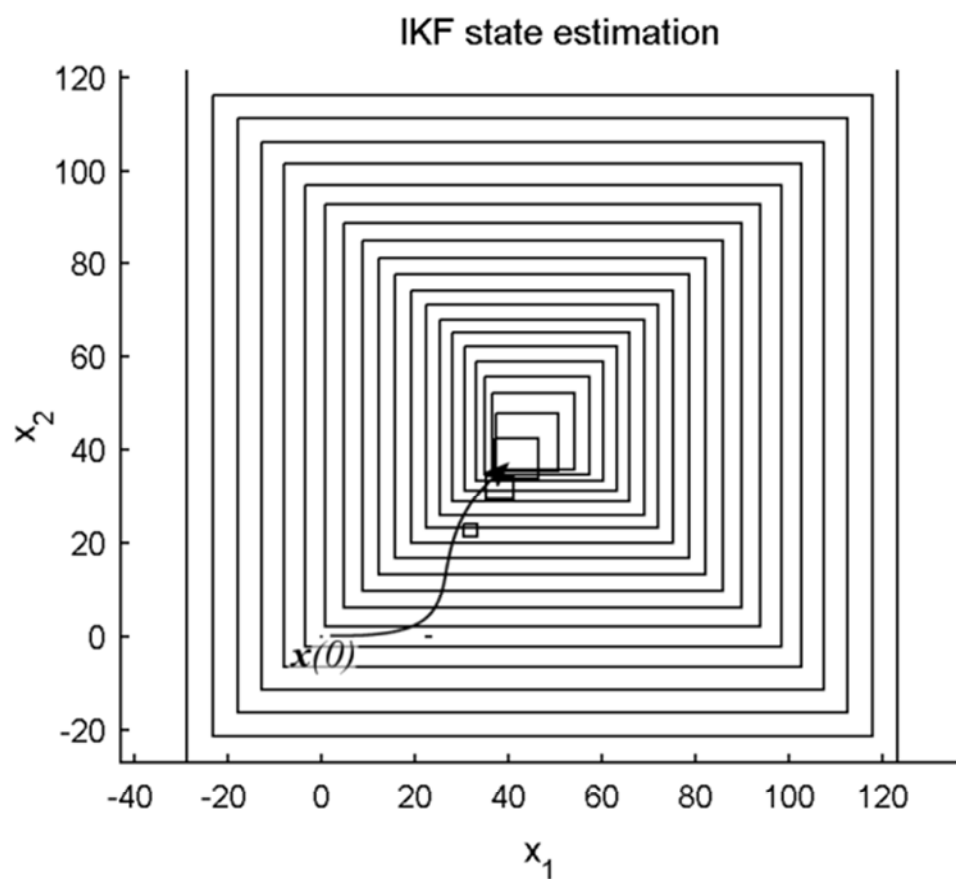


Figure 8(b). IKF estimates of the interval system state obtained using IA. Only the first 20 iterations shown, as the rectangles keep growing exponentially. The arrow follows the initial propagation of rectangular state enclosures.

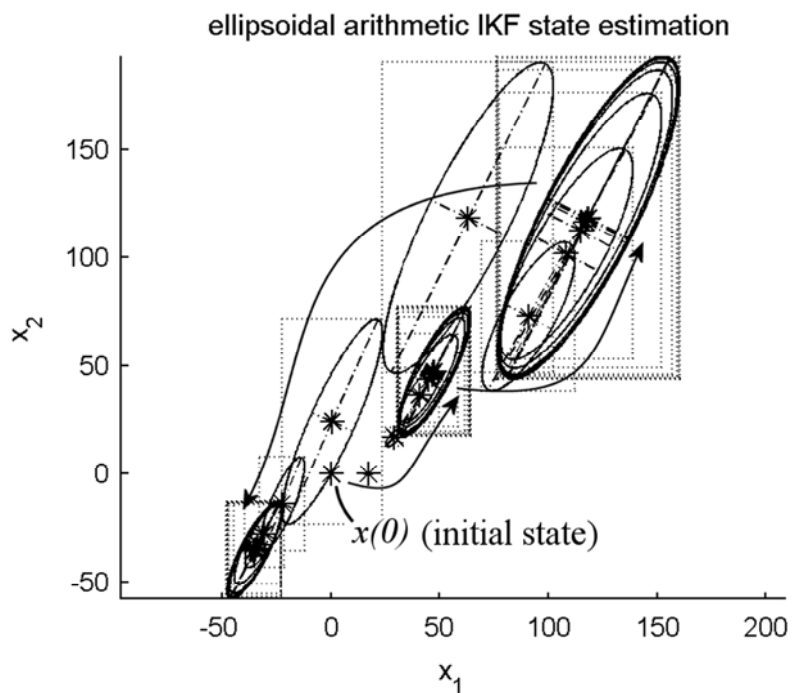


Figure 8(c). IKF estimates of the interval system state obtained using ellipsoidal arithmetic. The dotted rectangles correspond to the smallest box enclosure of each ellipse, but are not used for propagation.

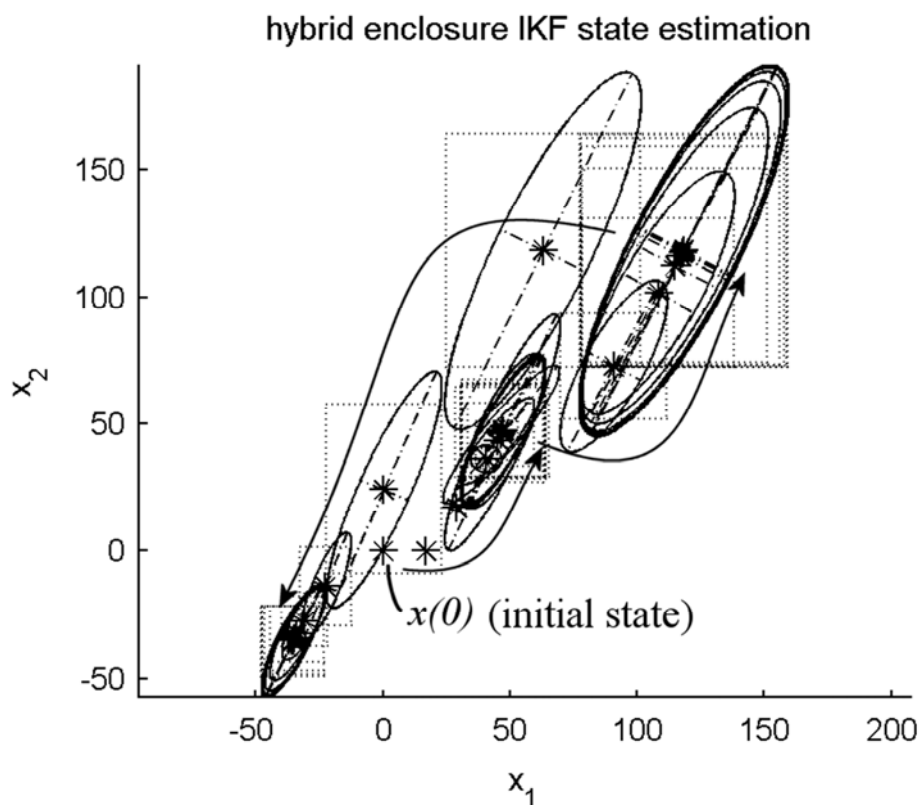


Figure 8(d). IKF estimates of the interval system state obtained using the hybrid enclosure algorithm. The dotted rectangles correspond to the box B_3 at each iteration.

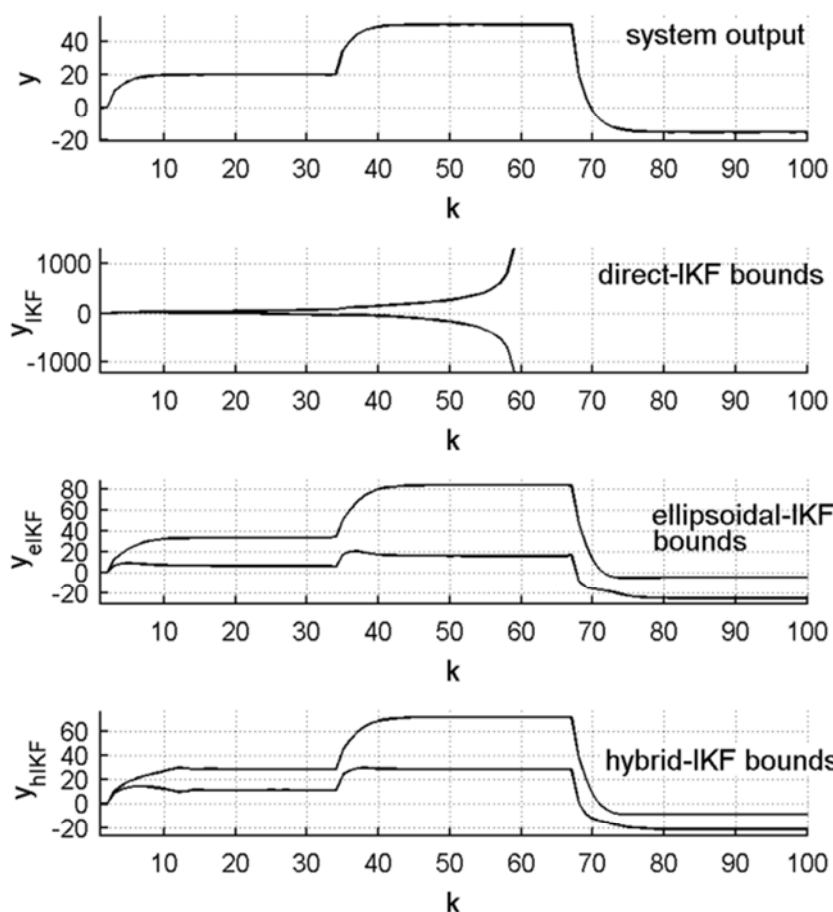


Figure 9. Output of the nominal underdamped system, and IKF bounds to the estimates of the output of the corresponding interval system using IA, ellipsoidal arithmetic, and hybrid enclosures respectively.

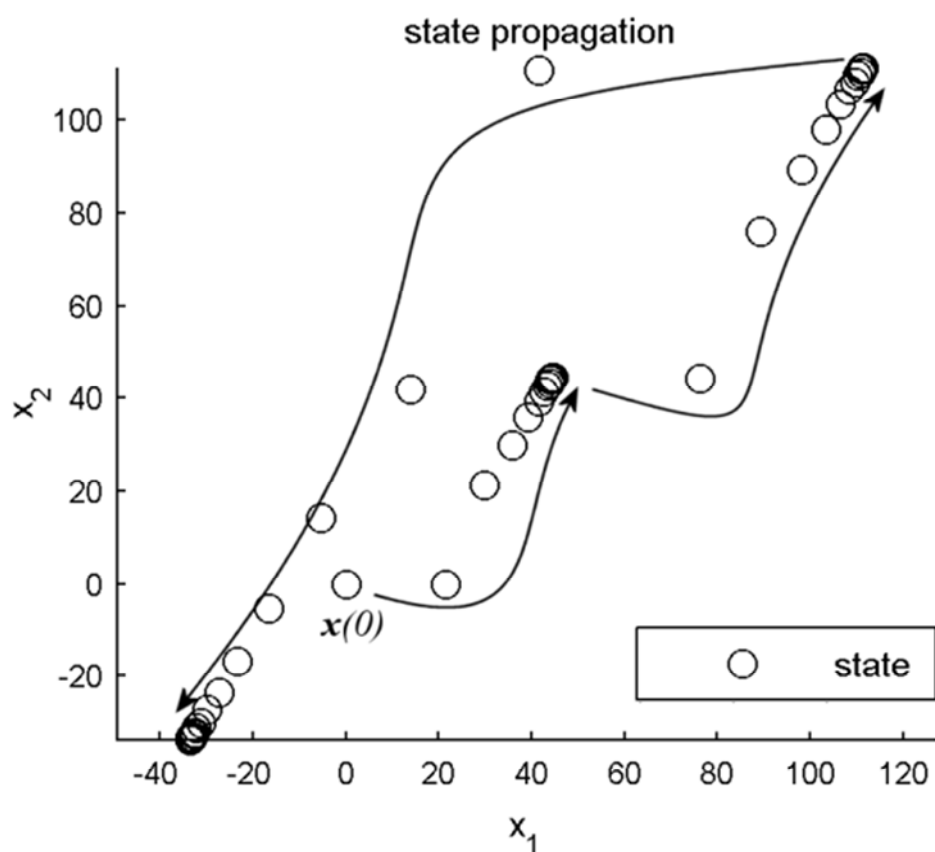


Figure 10(a). Simulation of the state-vector for the nominal overdamped system with poles at 0.5 and 0.1. States are depicted as circles for clarity, although they represent point-values.

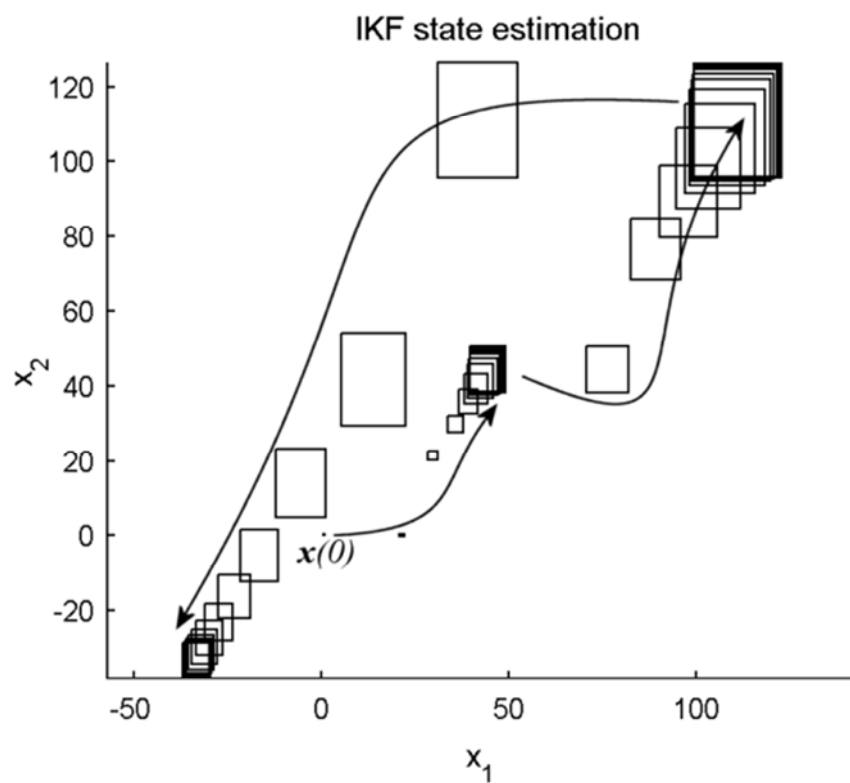


Figure 10(b). IKF estimates of the interval system state obtained using IA. The arrows indicate the direction of propagation of rectangular state enclosures.

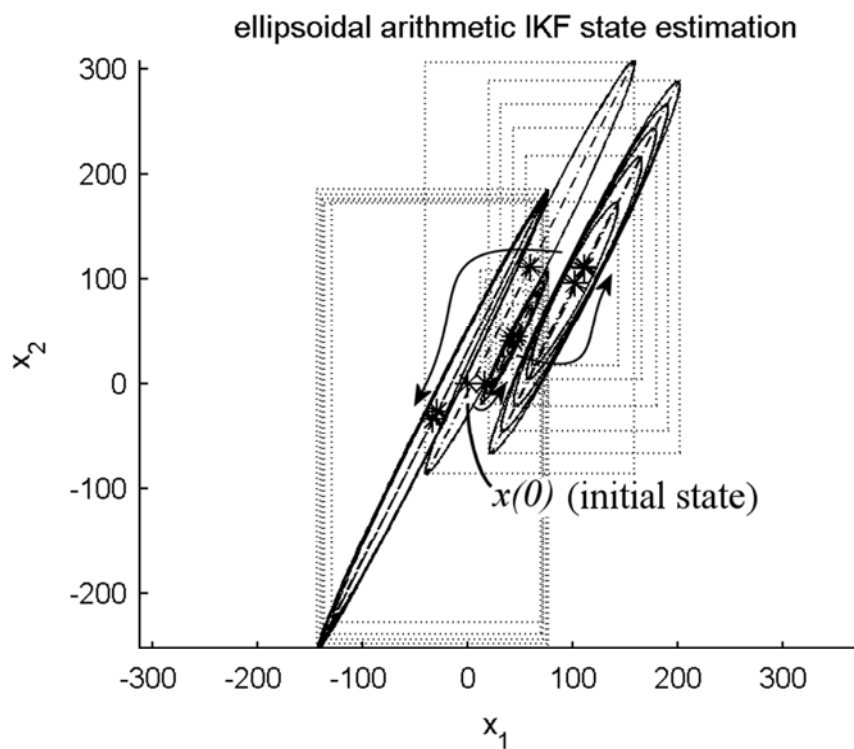


Figure 10(c). IKF estimates of the interval system state obtained using ellipsoidal arithmetic. The arrows indicate the direction of propagation of the state enclosures.

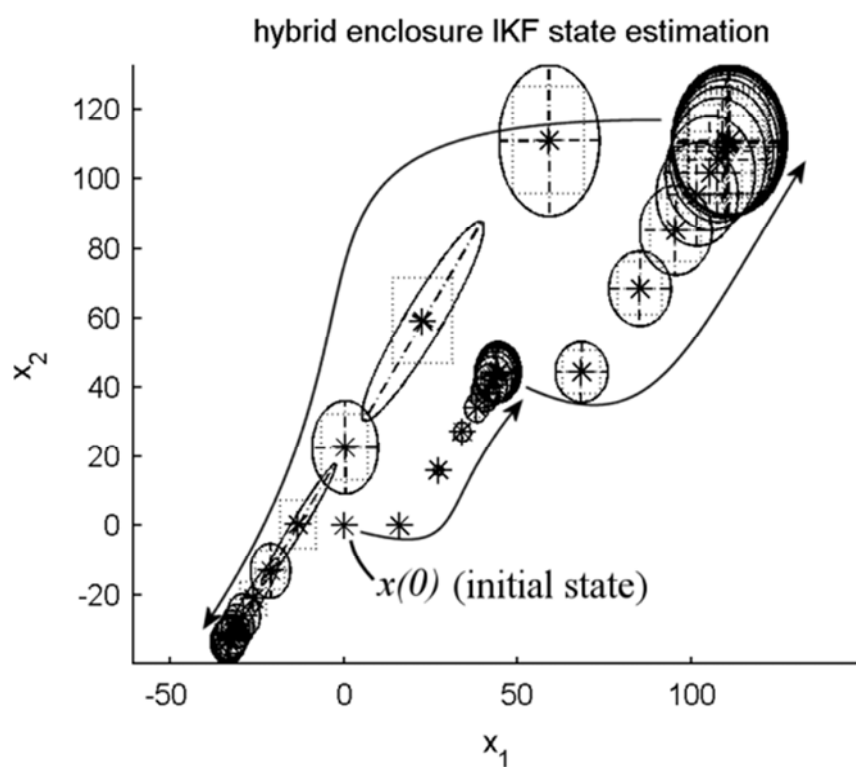


Figure 10(d). IKF estimates of the interval system state obtained using the hybrid enclosure algorithm. The arrows indicate the direction of propagation of the state enclosures.

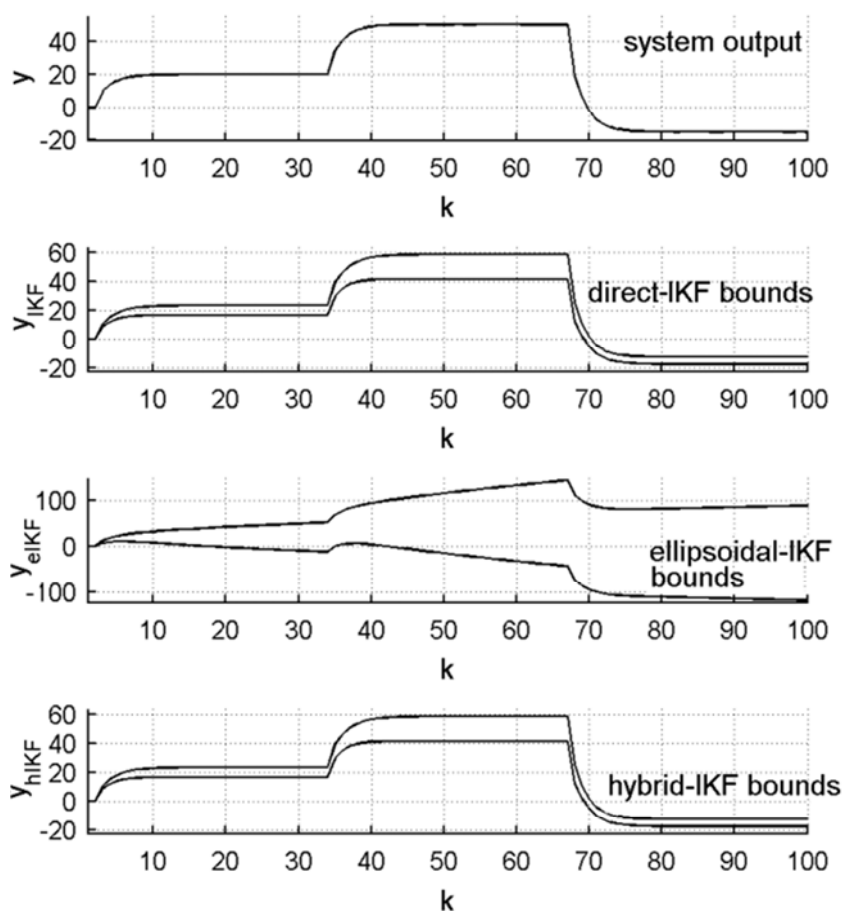


Figure 11. Output of the nominal overdamped system, and IKF bounds to the estimates of the output of the corresponding interval system using IA, ellipsoidal arithmetic, and hybrid enclosures respectively.